Journal of Applied Geophysics 110 (2014) 115–125

Contents lists available at ScienceDirect

Journal of Applied Geophysics

journal homepage: www.elsevier.com/locate/jappgeo

An efficient calibration procedure for correction of drift in EMI survey data

Samuël Delefortrie *, Philippe De Smedt, Timothy Saey, Ellen Van De Vijver, Marc Van Meirvenne

Research Group Soil Spatial Inventory Techniques, Department of Soil Management, Ghent University, Coupure links 653, 9000 Gent, Belgium

ARTICLE INFO

Article history:
Received 28 May 2014
Accepted 8 September 2014
Available online 18 September 2014

Keywords:
Electromagnetic induction
Drift correction
Spatial offset
Sensor calibration
Apparent electrical conductivity accuracy
In-phase susceptibility

ABSTRACT

Frequency domain electromagnetic induction (EMI) sensors with a small coil separation are used for near-surface surveys in a variety of domains. Regardless of the application, the instrument response(s) may suffer from a drift, meaning that a response at one given location may vary over time, despite no appreciable changes above or underneath the surface. Drift is unwanted as it may introduce global trends or abrupt changes in EMI data not related to the underground. In this paper, the effects of drift on the quadrature and in-phase responses of a ground-based system are researched by evaluating several multi-receiver EMI datasets. First, a stationary recording illustrates the need for a versatile drift compensation. For area surveys we propose an efficient drift correction procedure. To start, a calibration line that crosses the entire survey area within a short time frame is recorded. An approach to account for spatial offset between sensor midpoint and global navigation satellite system antenna is also detailed given the bearing it has on accurate localization. The residuals of coincident calibration and survey data can then be used to model and subtract the drift from the sensor data. This is performed by applying outlier detection and removal, followed by curve fitting of the comparison data. The developed procedure allows a near continuous evaluation of drift, without the need for ancillary data and is time efficient. The approach is shown to be suitable for various survey setups and drift effects.

1. Introduction

Frequency domain electromagnetic induction (EMI) sensors with a small coil separation are used for near-surface surveys in a variety of domains. An overview of advances and selected applications is given by Everett (2012). Regardless of the application, instrument response(s) may suffer from a drift with time, which is recognized as a systematic data error by Minsley et al. (2012) together with incorrect instrument calibration and improper data levelling. Signal drift can be visualized by performing a stationary recording (e.g. Gebbers et al. 2009), and is characterized as a systematic variation that exceeds the random signal noise over time, despite no appreciable changes above or underneath the surface. It is unwanted as it decreases the reliability of collected data: global trends and/or abrupt changes not related to the underground can be introduced in the data.

When the signal-to-noise ratio (S/N) is low, instrument drift becomes a critical disturbance since the magnitude may near the observed response (Grellier et al. 2013). Inversely, the error becomes less significant when the signal-to-noise ratio is high (Abdu et al. 2007). Yet even when the S/N is high, a relatively limited drift is unwanted given the high level of accuracy of modern instruments. Beamish (2011) states that the reference level of accuracy in apparent conductivity data may be less than 0.25 mS/m, though this is influenced by the sampling interval, instrument accuracy and survey setup.

The cause for signal drift is not unambiguous. Sudduth et al. (2001) performed various accuracy tests with an EMI sensor and inferred that ambient temperature variations could not be consistently related to drift. They suggested that drift may be the result of instrument instability integrated over time. Robinson et al. (2004) concluded that differential heating of EMI instruments is one factor contributing to drift. They also suggested that it may be caused by a combination of instrument factors such as circuit design, placement of temperature compensation sensors and coil performance under heating. It is noted that commercially available sensors may have an internal calibration procedure, which may account for (differential) temperature variations of the instrument. Nonetheless, signal drift remains possible in spite of internal calibration and technical advances.

The need to compensate for effects of drift has been recognized by several authors and different procedures for compensation have been developed:

- Robinson et al. (2004) recommended turning on the instrument 2 h ahead of surveying at the location as well as shading the sensor to limit (differential) heating. This approach is time consuming and the authors recognized that drift may only partially be corrected

* Corresponding author. Tel.: +32 9 264 58 69; fax: +32 9 264 62 47.
E-mail address: Samuel.Delefortrie@UGent.be (S. Delefortrie).

http://dx.doi.org/10.1016/j.jappgeo.2014.09.004
0926-9851/

for by field compensation. It was also suggested that the coil temperature may be recorded to exclude potentially inaccurate data. Abdu et al. (2007) likewise advocated field compensation such as shading the sensor and choosing a cooler day.

- Sudduth et al. (2001) and Abraham et al. (2006) proposed the use of repeat measurements at a fixed calibration point or transect during a survey for drift assessment and correction. Such an approach is time-consuming and results in a discrete evaluation of drift. If the evolution of drift is too sparsely logged or calculated (viewed over time), accurate compensation for an abrupt drift may not be possible.
- Use of a calibration line that crosses the entire survey area within a short time frame (Simpson et al. 2009). Comparison of coincident calibration and survey data (or cross-over points) can then be used to account for drift though methodological details have not been provided.
- Grellier et al. (2013) advocated use of calibration measurements every 5 to 20 measurements during a survey, at the then held position, to calculate drift offset. The calibration requires the instrument to be held 1.5 m above ground. Following, the ratio between apparent conductivity in horizontal coplanar orientation and vertical coplanar orientation is determined and the deviation with a known, correct ratio is calculated. They found that this method is considerably more efficient than performing repeat measurements at one location during a survey. However, the procedure is time-consuming.
- Procedures requiring other geophysical data (Deszcz-Pan et al. 1998; Minsley et al. 2012). However, such ancillary data are not always available.
- Filtering of survey data to account for systematic errors: data are processed after collection to conform to an expected statistical profile. This approach does not inform about the absolute value of drift, and does not discern between a trend caused by drift and a trend due to variation in the subsurface.

The drift correction procedure proposed in this paper aims at (1) a near continuous evaluation of drift of both quadrature-phase and in-phase responses for ground-based EMI data, without use of ancillary data or need of time consuming repeat measurements as well as (2) a drift compensation that is suitable for various drift effects and survey setups. For this purpose, a calibration line that crosses the entire survey area within a short time frame is employed. An approach to account for the spatial offset between sensor and global navigation satellite system (GNSS) is also detailed given the bearing it has on accurate localization. Comparison of coincident calibration and survey data can then be used to model and subtract the drift. This is performed by applying outlier detection and removal, followed by curve fitting of the residuals between the calibration and survey data. Suitability for different survey setups and drift effects is examined, and the benefits and drawbacks of the procedure are discussed.

All data processing was done in Matlab (The Mathworks Inc, Natick, USA). The Matlab code developed for this paper is freely available from the corresponding author at request.

2. Materials and methods

2.1. EMI instrument and setup

EMI instruments produce a time-varying electromagnetic field, thereby inducing EM fields in the subsurface and measure the resulting field, which has a quadrature-phase (QP) component and in-phase (IP) component, expressed in parts per thousand (ppt).

The QP response was converted to apparent electrical conductivity (ECa), expressed as mS/m, using the formula (McNeill 1980):

$$\mathrm{ECa} = \frac{2}{\pi\ f\ s^2\ \mu_0} \cdot \left(\frac{\mathbf{H}_s}{\mathbf{H}_p}\right)_{QP}$$

where f is the frequency (Hz), s is the coil separation (m), μ_0 is the magnetic permeability of free space ($4\ \pi\ 10^{-7}$ H m^{-1}) and $(\mathbf{H}_s/\mathbf{H}_p)_{QP}$ is the QP component of the secondary $\mathbf{H}_s$ to primary $\mathbf{H}_p$ magnetic field coupling ratio. This formula is an approximation based on the assumption of operating the instrument in a low induction number (LIN) environment with zero instrument elevation.

Multi-receiver EMI data were collected using a DUALEM 21S sensor (DUALEM Inc., Milton, Canada), which has an operating frequency of 9 kHz and four coil configurations: one transmitting coil paired with four receiving coils of which two perpendicular (PRP) coil configurations with 1.1 and 2.1 m intercoil spacings (11PRP and 21PRP) and two horizontal coplanar (HCP) coil configurations with an intercoil spacing of 1 and 2 m (1HCP and 2HCP) respectively. By housing several coil configurations, near simultaneous readings of different subsurface volumes can be collected (e.g. Saey et al. 2014).

For surveying, the sensor was positioned in a polyethylene sled that completely encased the instrument. The instrument elevation (intercoil centre line) was 0.16 m and the sampling frequency was 8 Hz (for each coil configuration). For area investigation, the sled was towed by an all-terrain vehicle (ATV) by use of a flexible connection (two ropes). The sled ran parallel to the driving direction and the offset between the front of the sensor and the vehicle was around 3.5 m. Geographic coordinates were logged using a differential GPS (dGPS) system which was located on the vehicle. GPS data and sensor responses were logged synchronously at 1 Hz and 8 Hz respectively. When performing the stationary recording, the instrument was located in an open field, with no power lines or leads above the surface or underground to minimize ambient interference.

2.2. Study areas

All data were collected in Belgium. The stationary measurement (central coordinates X: 554 695 m and Y: 5 675 937 m—UTM 31 geographic coordinate system) was performed on 14 March 2014 during warm and sunny conditions. The details of the area surveys are listed in Table 1.

The subsurface of all survey areas is characterized by unconsolidated, Quaternary sediments overlying unconsolidated, Pleistocene deposits. The study area at Koolkerke is farming land and the soil layer textures range from sand to clayey sand. Generally, the conductivity of the subsurface is low. The survey area at Veurne is cultivated land and the soil layer textures range from clay to loamy sand. The area surveyed in Raversijde is located on the beach, within the intertidal zone. The subsurface consists of clastic (beach sands and fine-grained mudflat sediments) and biogenic (peat) deposits. Owing to the saline groundwater (due to mixing with sea water), both the ECa and IP responses are strongly elevated and the S/N ratio is high (Delefortrie et al. 2014).

2.3. Data processing

2.3.1. Shift correction

After collection, the ECa and IP data were corrected for the spatial offset between the intercoil centres for each coil configuration and the dGPS system, which was mounted on the vehicle at the same place as the flexible connection, making necessary only an in-line shift of the coordinates. Fig. 1 summarizes the applied routine. WGS84 spherical coordinates were logged and transformed to Cartesian coordinates in the UTM geographic coordinate system. Coordinates were then assigned to the sensor data by interpolating the XY coordinates through use of a piecewise cubic interpolation on basis of time (t). Following, the distances between subsequent data points (time-wise) were calculated and the cumulative distances were calculated. The shift was subtracted from the cumulative data. Finding the closest values and their indices between the cumulative distance and the cumulative distance minus shift, then enables to assign shifted coordinates to the sensor data.

Table 1
Survey details. The Cartesian coordinates are in the UTM geographic coordinate system.

	Koolkerke	Veurne	Raversijde
Date	09 April 2013	06 October 2013	26 January 2012 and 12 March 2012
Central coordinates [m]	X: 517 685 Y: 5 676 855	X: 478 700 Y: 5 658 143	X: 489 150 Y: 5 672 425
Surface area [ha]	1.3	3.5	6.8
Survey duration [h]	1.3	4.8	5
Calibration line duration [min]	4	5	5
Calibration line moment	Start survey, 20 min after turning on sensor	Start survey, 30 min after turning on sensor	Start survey, 20 min after turning on sensor
Distance between parallel lines [m]	2	1	2
Operating speed [m/s]	2.2–2.8	2.2	2.2–2.8
Weather conditions	Cloudy and rainy	Cloudy and dry	Day 1: cloudy and rainy Day 2: clear and sunny
Median 11PRP ECa [mS/m]	9	18	535
Median 11PRP IP [ppt]	−0.4	−0.25	0.2

Because shifted coordinates are searched only between existing coordinate points, accuracy may be low. Synthetic time data should therefore be added to the sensor data (before the piecewise cubic interpolation) to remedy this. The smaller the time step (e.g. 0.01 s) of the synthetic data, the higher the accuracy. Additionally, it is good practice to delete inaccurate and/or duplicate GNSS data (e.g. within less than 10 cm of each other) before applying the shift correction and to disregard the first points where the cumulative distance minus the shift is negative. It is noted that the procedure assumes that the sled always follows the GNSS track. This assumption is valid when driving in a straight line but can be erroneous when tight turns are made.

2.3.2. Time series processing

Removal of duplicate points is an important step prior to working with time series. Duplicate points of the area survey datasets were removed by requiring subsequent points (viewed in time) to be at

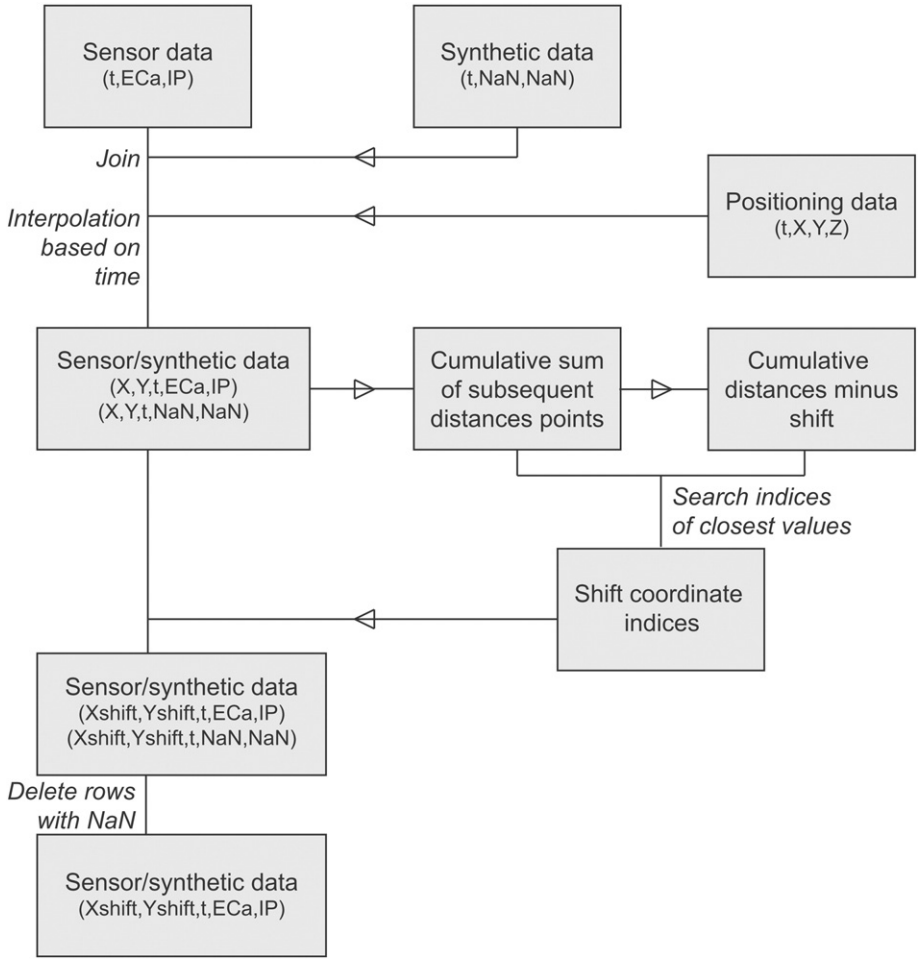

Fig. 1. Flowchart summarizing the applied routine for correcting spatial offset between instrument and dGPS system. X and Y denote X and Y Cartesian coordinates, t denotes time and NaN stands for not a number, which is a no-data identifier.

least 6 cm apart. Afterwards, the initial time was set to zero and only time intervals were kept.

A Hampel filter is a moving window, nonlinear filter that detects local outliers in a time-series. These can then be deleted or replaced by the local median. The code used for applying the filter can be found in Nielsen (2012). A faster alternative is provided by Smith (2013). Input parameters are half-width of the filter window and a threshold to determine upper and lower bounds outside of which point data are considered outliers. A half window width of 360 s was used as well as a threshold of 3. More details about the Hampel filter can be found in Pearson (2002). By comparing the Hampel filter with moving average or median filters applied to several EMI datasets, it was found that is generally more suitable for noisy time series with sudden breaks or erratic behaviour.

B-splines are spline functions constructed from polynomial pieces, joined at certain values of x (time, when working with time series), the knots or spline breaks. Once the breaks are given, the B-splines can be computed recursively, for any desired degree of the polynomial.

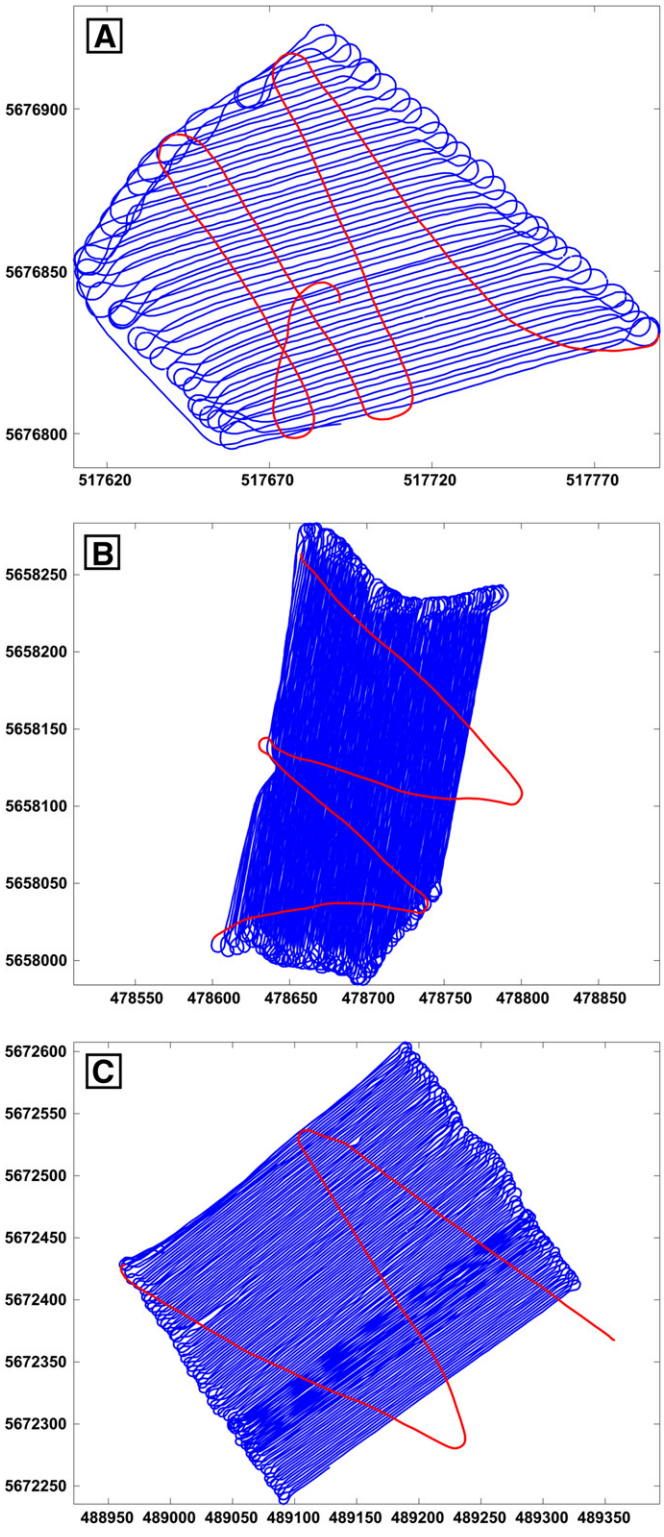

Fig. 2. Calibration data (red) and survey data (blue) of the data collected at (A) Koolkerke, (B) Veurne and (C) Raversijde. The axis scaling is different for each survey area.

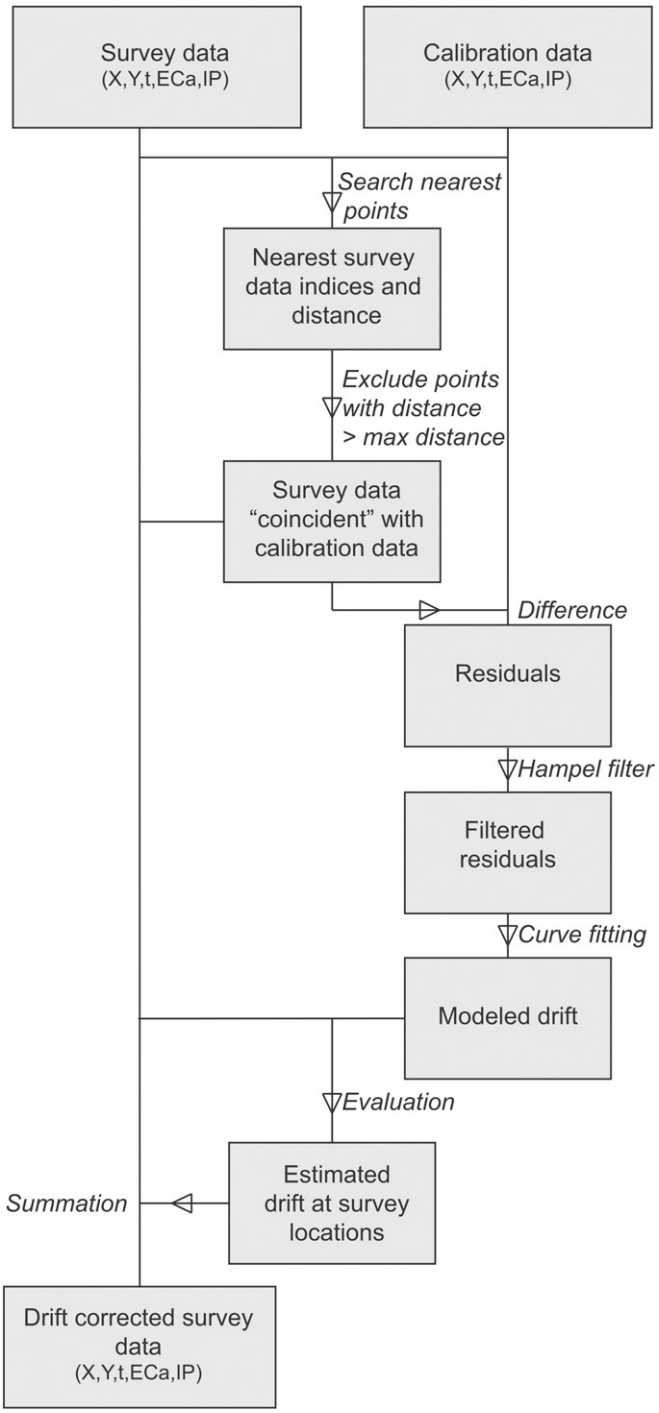

Fig. 3. Flowchart summarizing the proposed routine for drift compensation.

A short overview of B-splines and their construction can be found in Eilers and Marx (1996). The code used for the curve fitting by use of B-splines can be found in Lundgren (2010). The B-spline fitting of the residual data in the results was done by user specification (number of breaks or time of breaks and order of the polynomial).

2.3.3. Drift correction

To warrant an accurate drift correction, the execution of the calibration line has to be conceptually sound. It should: (i) cross the entire survey area, preferably in the shape of a 'w' to achieve a good balance between area coverage and time as shown in Fig. 2, (ii) allow comparison over the entire survey time range, (iii) be kept as brief as possible (e.g. <10 min), (iv) be executed at a low, constant speed (e.g. 2 m/s) and (v) preferably be performed when the instrument has had a sufficiently long 'warm-up' (e.g. 20 min).

Measurements recorded at the same place at different times might deviate due to signal drift. Instrument noise, which ambient interference may exacerbate, contributes to calculated differences as well. Data accuracies can be improved by increasing the sampling interval though for mobile operation a sufficiently small sampling interval may be preferred (e.g. 8 Hz). Since drift is a systematic error it may be recognized as a pattern exceeding the instrument noise level. However, other sources of deviation between the calibration and survey data (in addition to instrument noise) also occur.

Positional accuracy of the measurements affects the comparison of calibration and survey points. If there is a spatial offset between sensor and dGPS antenna an accurate shift correction is crucial. The correction applied was performed as described in the Materials and methods section. However, corrections for spatial offset can include movement parameters such as velocity or travelling direction since the sensor may not follow the antenna track in tight vehicle turns (e.g. Gottfried et al. 2012). As this area is usually not very relevant for the drift correction itself, the correction applied was deemed adequate.

As it is opportune to have sufficient comparison points, the comparison must not be limited to coincident points. Rather, a search window around the calibration points may be used. It follows that small-scale, subsurface heterogeneity may be a cause for discrepancy. A search window of 0.5 m was used for all datasets.

Fig. 2 shows that the direction of the sensor is not equal for coincident survey and calibration points. Difference in orientation of the instrument at coincident points is another cause for discrepancy and may even give rise to extreme outliers (e.g. above underground metallic objects). Furthermore, topography may exacerbate differences: aside from a difference in planar direction it may give rise to a difference in the pitch and roll of the sensor.

Aforementioned causes for the difference between the calibration and survey data can stack and introduce greater uncertainty to the drift evaluation (exceeding instrument noise levels). When comparing calibration and survey data, systematic variations are caused by drift and can only be modelled when such change can be discerned. If enough comparison locations are present, it is assumed that the actual drift is best characterized by fitting a smooth, polynomial curve to the comparison points. Thus, to model and subtract the drift outlier removal and curve fitting are recommended.

Fig. 3 summarizes the drift correction procedure. The correction consists in comparing the instrument responses at every calibration point and the survey points within a specified (circular) search window. The time of the survey data is stored, the difference in response(s) of survey and calibration data are calculated, and this is performed for all calibration points. Outlier detection, curve fitting and visualization of the residuals (a time series) are then possible. When spline fitting, the number of spline breaks or the exact location of the breaks is entered or pre-set as

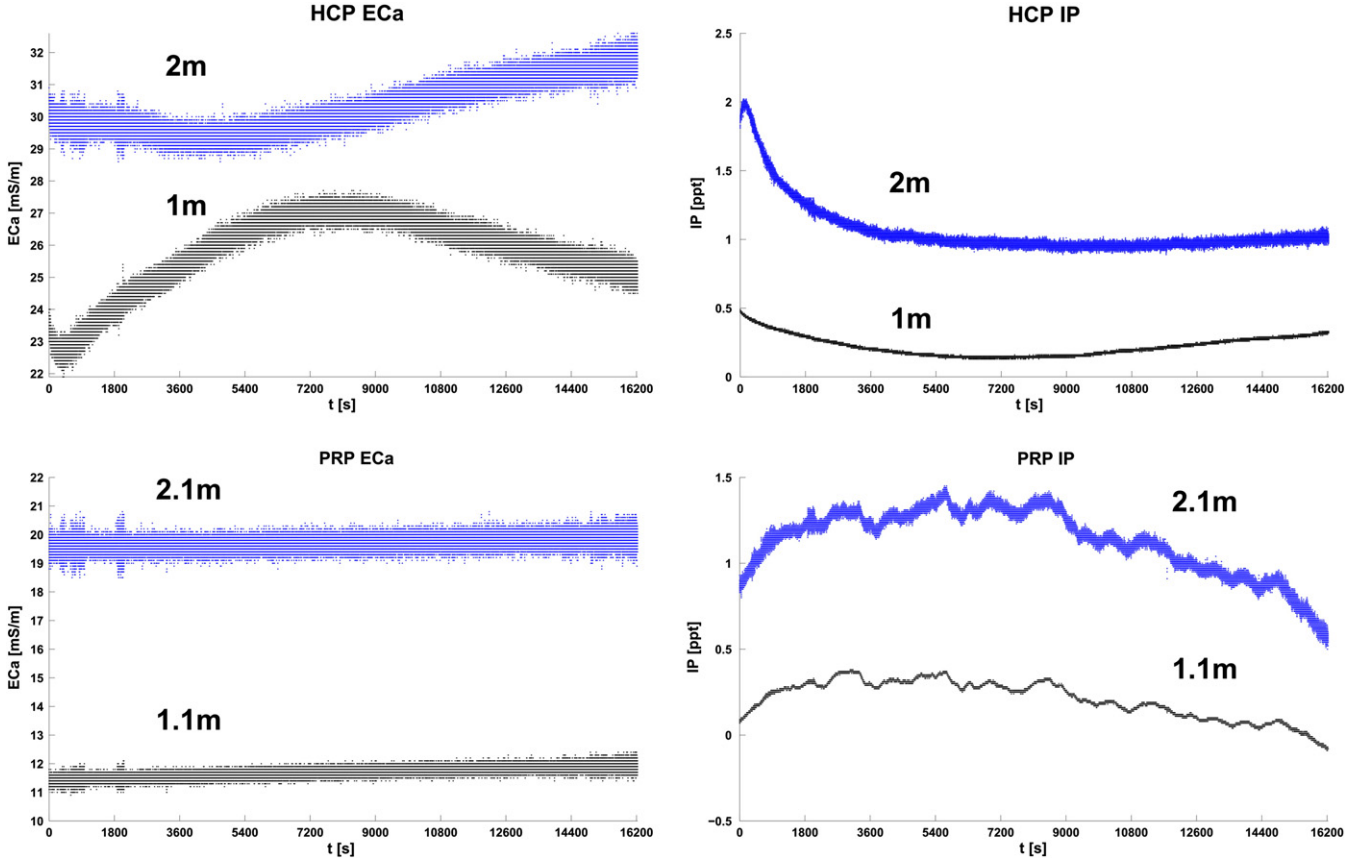

Fig. 4. A 4.5 h stationary recording at Hoeke for the DUALEM 21S responses (129 600 measurement points for each response). The uppermost curves (black) are the 2 or 2.1 m coil configurations whilst the lower most curves (blue) are the 1 or 1.1 m coil configurations. The QP responses have been converted to ECa using the LIN approximation which has linearly scaled the noise levels.

Table 2
Averaged local ranges (moving time window of 10 s) for the stationary recording data (sampling interval of 8 Hz). These values are an indication of the coil configuration noise levels.

	ECa (mS/m)	QP (ppt)	IP (ppt)
1HCP	0.8	0.01	0.02
11PRP	0.5	0.01	0.01
2HCP	1.0	0.07	0.07
21PRP	0.9	0.07	0.07

well as the order of the spline. The modelled drift can then be evaluated at every survey measurement (based on its time) and corrected for. A maximum distance of 0.5 m from the calibration points, with a maximum of 5 nearest neighbours, was used for selecting the data pairs to be compared.

It is important to have a good understanding of the vertical scale when assessing drift. Outliers may complicate this and can adversely affect the fit when modelling drift by use of B-splines. Where they should be removed, a Hampel filter offers an adequate solution. The moving window filter also allows visualizing nominal data, which is similar to a local median for the time series. This nominal data may be equated to the estimated drift and can be evaluated for all survey points by linear interpolation. This can provide a fully automated drift correction. Nonetheless, the use of curve fitting is preferred since it allows more flexibility and user control. It is also noted that extrapolation of the nominal data is not justifiable.

3. Results

3.1. Stationary measurements

The temporal variation of instrument response, at a fixed location, is visualized in Fig. 4. It is apparent that some (DUALEM) responses are more stable than others:

- The PRP ECa responses are very stable, showing no or limited, linear drift.
- The HCP ECa and IP responses show a quadratic trend with time. The greatest instability is encountered right after powering the sensor and complete stabilization with time may or may not occur.
- The PRP IP responses are rather unstable and show erratic behaviour.

Other stationary recordings have shown similar results and it follows that the drift of a coil configuration can be characterized. It is also clear that a drift correction procedure has to be flexible since there are a wide range of drift effects (linear, quadratic and/or periodic trends as well as erratic behaviour).

To evaluate the noise levels of the signals, a moving window of 10 s was utilised to calculate local ranges over the time series. These were then averaged to represent the noise levels (Table 2). It is noted that noise levels are influenced by ambient interference and by the sampling interval. Furthermore, it is clear that the noise level increases with increasing coil separation.

The main premise of the proposed drift correction is that the calibration data does not suffer from signal drift, or rather, that signal drift does not exceed instrument noise, given a small enough time window. The data suggest that this premise is viable for a five minute calibration line recording. Generally, the variation does not exceed the noise level in such a small time interval. However, performing the calibration line immediately after powering the instrument should be avoided, given that the greatest signal instability is usually encountered in this moment.

3.2. Application of drift correction procedure

Fig. 5 exemplifies the use of the Hampel filter for 11PRP IP data collected at Koolkerke. All points outside the bounds are considered outliers. The plot shows that differences in response can be very large, due to high contrasting small-scale anomalies and/or presence of metal. Metal objects, especially, may give rise to a vastly differing response when the orientation and position of the sensor differ. On all subsequent plots, outlier detection and removal were performed.

The comparison of calibration and survey data as well as the modelled drift for the Koolkerke dataset is visualized in Figs. 6 and 7. Similarly to the stationary recordings, PRP ECa drift is characterized by linear trends whereas the HCP ECa and IP drift are characterized as quadratic trends. The 21PRP IP response is not shown as it suffered from severe noise and instability, rendering the signal of little use; see also De Smedt et al. (2013). Contrarily, the 11PRP IP response was found to be sufficiently stable. The local range of the residuals is usually around one to three times the noise level of a response.

An initial difference of zero is expected for the residuals if the calibration line was performed just before collecting the survey data. If this is not the case, the validity of the correction is compromised.

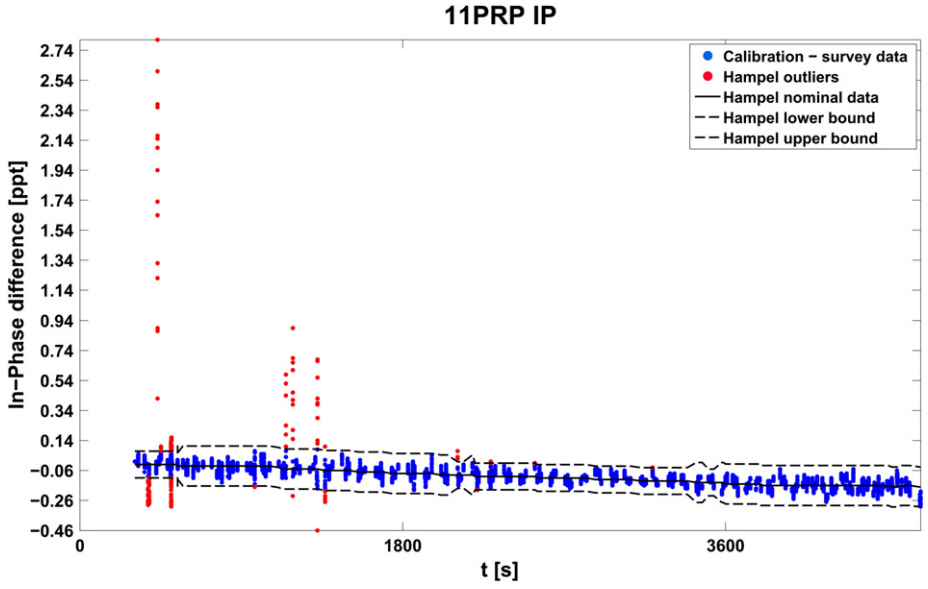

Fig. 5. Calibration and survey data residuals for the 11PRP IP response at Koolkerke with Hampel filter outlier detection, nominal data and upper and lower bounds.

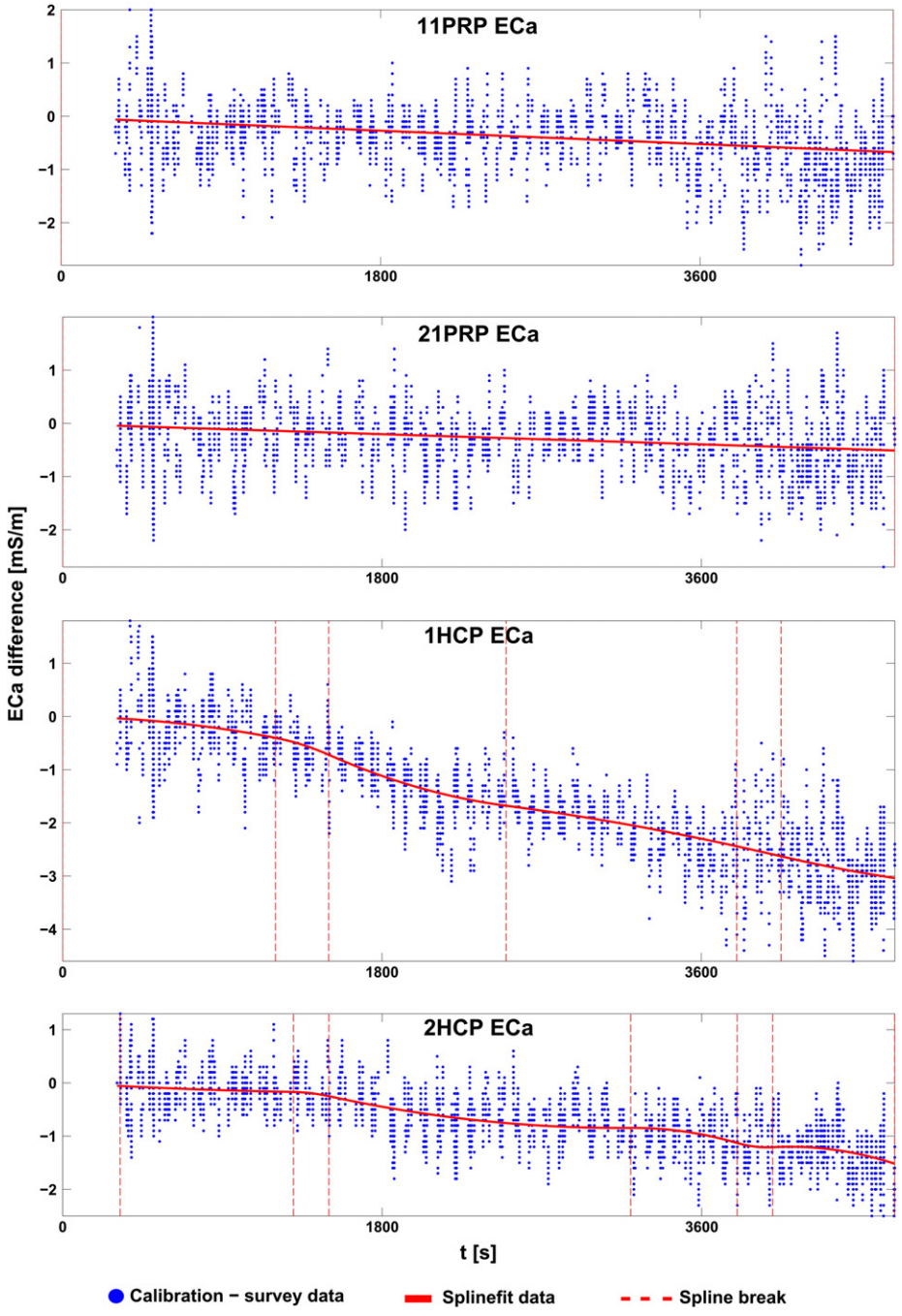

Fig. 6. Calibration and survey data residuals for the ECa responses at Koolkerke as well as the modelled drift by means of spline fitting. The Y-axis scaling is the same for all responses.

However, all modelled drift (as well as the Hampel nominal data) starts at a difference of (nearly) zero, advocating the validity of the approach.

A drift of 3 mS/m per hour is observed for the 1HCP ECa response, which is significant considering the low conductive subsurface (Fig. 8), whereas the modelled 21PRP ECa drift remains within the noise level of the response. It follows that a drift correction is not always necessary. Nonetheless, the need for drift compensation can be evaluated only when the drift is assessed. It is noted that when only some signals are significantly affected by drift, this poses a problem for processing that involves combination of the signals (e.g. principal component analysis of the signals).

Drift patterns for the Veurne dataset were similar to the drift patterns of the Koolkerke dataset. However, the 11PRP IP response suffered from instability and shows a complex variation with time. Fig. 9 visualizes the 11PRP IP comparison data and the measurements without and with drift compensation applied. It is clear that the broad bands, caused by instability of the signal, are compensated for.

At Raversijde, the tides made necessary data collection over the course of two days. During the first survey, a calibration line was performed for the entire study area. The data collected during the second survey partially overlapped with the first survey data (see Fig. 10). By comparing both data sets with the calibration line, it was possible to assess drift for the entire survey area. To this end, the time lapse between the surveys was reset to zero. At the moment the data from the second survey starts a sudden jump can be seen in the comparison data, allowing to simultaneously drift correct and synchronize the data. This is another advantage to performing a calibration line that covers the entire study area. Where the difference in ECa in the zone of overlap is clear in the non-drift corrected data, these data are synchronized after summation with the modelled drift.

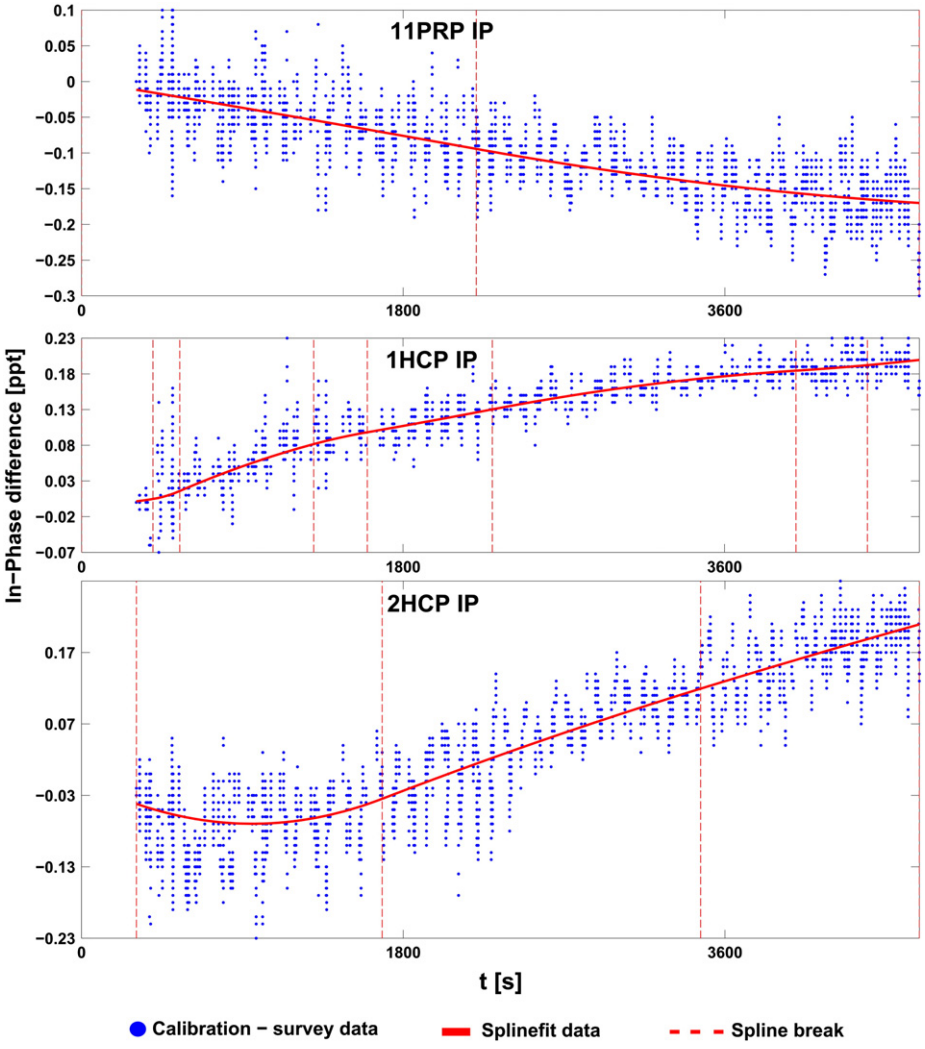

Fig. 7. Calibration and survey data residuals for the IP responses at Koolkerke as well as the modelled drift by means of spline fitting. The Y-axis scaling is the same for all responses.

4. Discussion

The crux of the proposed drift correction is that a calibration line covering the survey area, performed in a sufficiently short amount of time, does not suffer from significant drift. The data presented suggests that this generally holds true, yet performing the calibration line immediately after powering the instrument should be avoided. If a systematic variation is discerned in the comparison of survey data with such a calibration line, drift can be compensated for. However, the comparison data is subject to various, random errors necessitating calculation of nominal data and/or use of curve fitting to model the signal drift. Nonetheless, a near continuous evaluation is preferred as results show that drift may be erratic. Additionally, a drift compensation procedure has to be versatile, especially considering real survey conditions: ambient temperatures may vary strongly, there may be unplanned pauses between measurements and restarting or replacing the sensor during a survey (causing recalibration) may be necessary. Furthermore, it may be unfeasible to frequently return to a given location or collect a lot of ancillary data in order to correct for signal drift. For all the aforementioned reasons the proposed drift correction is a boon, allowing to maximize the reliability of collected data and allowing flexibility for varying drift situations and problems. For instance, a calibration line can be performed at a later time should data be corrupt or lacking.

In utilising the drift procedure it should be assessed if the desired accuracy can be reached. Compensation for drift that is smaller in magnitude than instrument noise level is possible, though often not achievable. It is noted that correcting for high (random) noise levels is not possible using the described method: a sufficiently stable signal (in the sense of low stochastic noise) was postulated. Furthermore, the calibration line must be well conceived.

Although the presented approach was applied to only one type of EMI sensor and four possible coil configurations, the correction is generally applicable and expeditious. It is good practice to log several stationary recordings during different atmospheric conditions to assess which instrument responses are prone to drift and whether the drift may be characterized (e.g. consistent observation of a linear drift for the DUALEM ECa PRP responses). Such a priori knowledge may then be used in modelling the signal drift by curve fitting, especially if the process is fully automated.

The approach described holds additional advantages. Synchronization of data collected at different times is possible through the use of a single calibration line though a sufficiently high sampling frequency is required. Enough comparison locations are necessary since the differences between calibration line and survey data are not solely due to drift and since drift may be abrupt. Too few comparison points over time may preclude accurate drift correction. However, as the highest obtainable sampling frequency keeps rising with continual instrumental developments, a drift compensation procedure as described herein may only become increasingly relevant with time.

It is noted that a similar use of a calibration line has been employed in a variety of domains. Siemon (2009) examined its use for the levelling

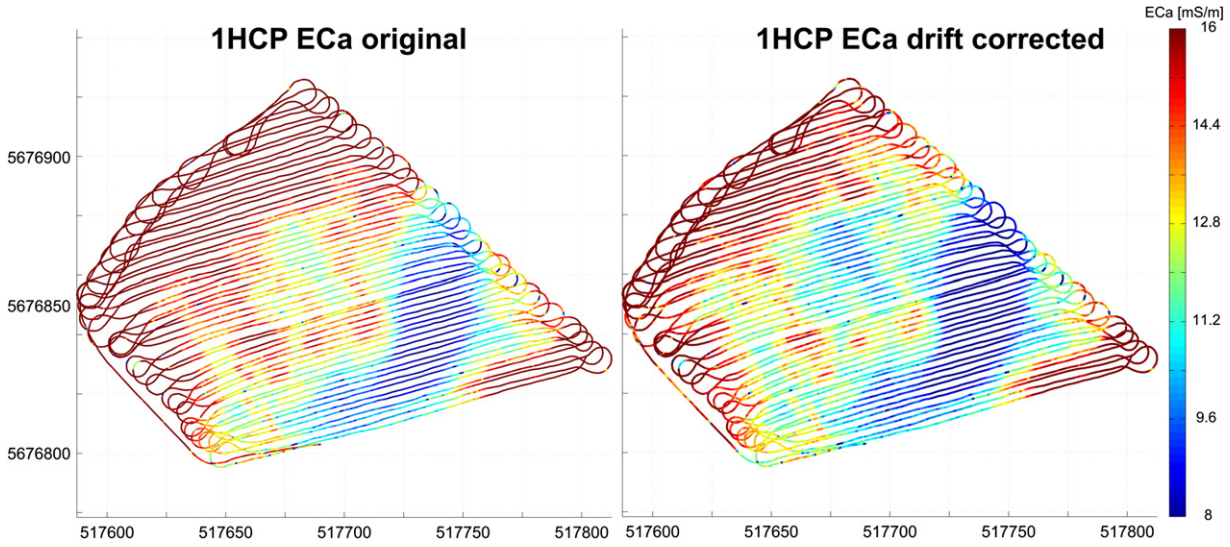

Fig. 8. 1HCP ECa scatter plots of the non-drift corrected data (left) and the drift corrected data (right) of the Koolkerke dataset.

of helicopter EM data and found that tie-line levelling is often not useful when applied to QP or IP instrument data because they are nonlinearly dependent on the instrument altitude. This is clearly not the case with ground-based EM data, which does not suffer from elevation offsets at cross-over points. We also note that applying the drift correction procedure to the QP or LIN ECa data is essentially the same for our system

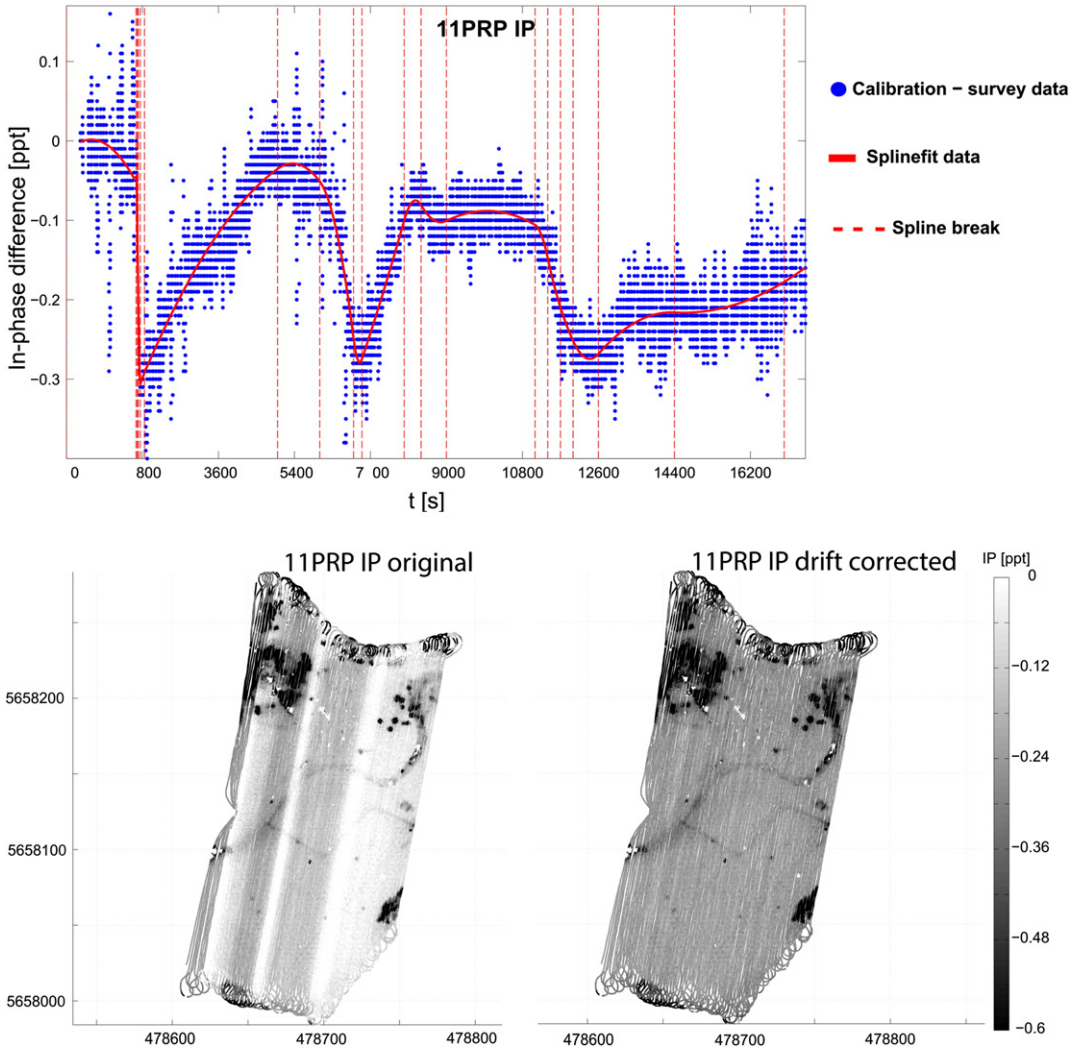

Fig. 9. Top: Calibration and survey data residuals for the 11PRP IP response at Veurne as well as the modelled drift by means of spline fitting. Bottom: 11PRP IP scatter plots of the non-drift corrected data (left) and the drift corrected data (right).

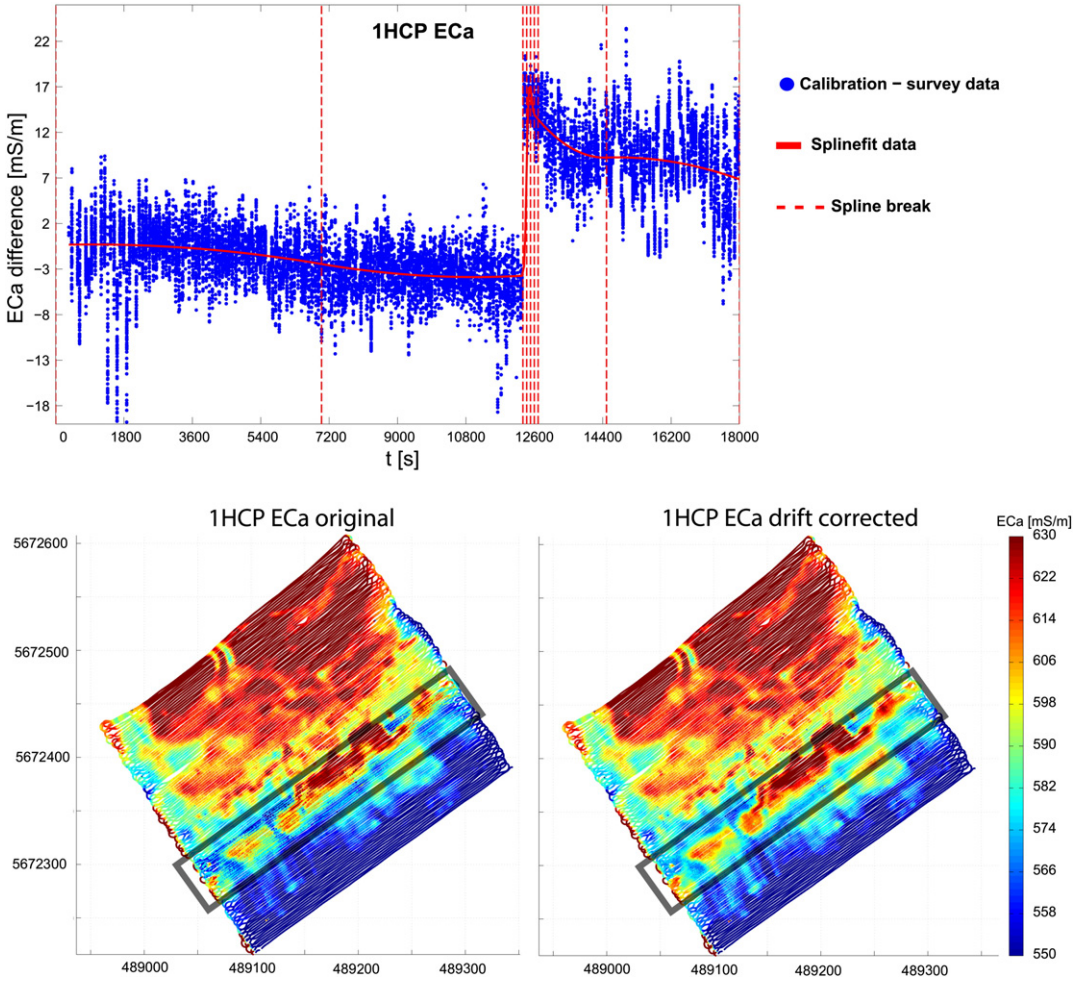

Fig. 10. Top: Calibration and survey data residuals for the 1HCP ECa response at Raversijde as well as the modelled drift by means of spline fitting. Bottom: 1HCP ECa scatter plots of the non-drift corrected data (left) and the drift corrected data (right). The black rectangular zone is the zone with data overlap between the two surveys.

because of the linear approximation. This shows that what is a good practice for land-based systems is not necessarily a good practice for other EM systems.

5. Conclusions

By using the drift procedure detailed herein, a relative compensation with regards to the (stable) calibration data is performed. Whilst signal stability can be achieved in this manner, an absolute calibration is not realized. This means that multiple calibration lines will give rise to different results and whether this is due to changes in temperature, other physical parameters or due to absolute calibration is not easily distinguished between. However, given the results obtained, the procedure is for all intents and purposes an excellent first step in processing EMI data as it allows maximizing the reliability of collected data with regards to signal stability.

Acknowledgments

We would like to thank Valentijn Van Parys for his support and help on the field. The survey at Veurne was commissioned and funded by the West Flanders Intermunicipal Association (WVI). Philippe De Smedt is a Postdoctoral Fellow of the Research Foundation—Flanders (FWO), research grant: FWO13/PDO/046. We are grateful to one anonymous journal reviewer.

References

Abdu, H., Robinson, D.A., Jones, S.B., 2007. Comparing bulk soil electrical conductivity determination using the DUALEM-1S and EM38-DD electromagnetic induction instruments. Soil Sci. Soc. Am. J. 71, 189–196. http://dx.doi.org/10.2136/sssaj2005.0394.

Abraham, J.D., Deszcz-Pan, M., Fitterman, D.V., Burton, B.L., 2006. Use of a handheld broadband EM induction system for deriving resistivity depth images. Symposium on the Application of Geophysics to Engineering and Environmental Problems, pp. 1782–1799.

Beamish, D., 2011. Low induction number, ground conductivity meters: a correction procedure in the absence of magnetic effects. J. Appl. Geophys. 75, 244–253.

De Smedt, P., Saey, T., Meerschman, E., De Reu, J., De Clercq, W., Van Meirvenne, M., 2013. Comparing apparent magnetic susceptibility measurements of a multi-receiver EMI sensor with topsoil and profile magnetic susceptibility data over weak magnetic anomalies. Archaeol. Prospect. 21, 103–112. http://dx.doi.org/10.1002/arp.1467.

Delefortrie, S., Saey, T., Van De Vijver, E., De Smedt, P., Missiaen, T., Demerre, I., Van Meirvenne, M., 2014. Frequency domain electromagnetic induction survey in the intertidal zone: limitations of low-induction-number and depth of exploration. J. Appl. Geophys. 100, 14–22. http://dx.doi.org/10.1016/j.jappgeo.2013.10.005.

Deszcz-Pan, M., Fitterman, D.V., Labson, V.F., 1998. Reduction of inversion errors in helicopter EM data using auxiliary information. Explor. Geophys. 29, 142–146.

Eilers, P.H.C., Marx, B.D., 1996. Flexible smoothing with B-splines and penalties. Stat. Sci. 11, 89–121.

Everett, M.E., 2012. Theoretical developments in electromagnetic induction geophysics with selected applications in the near surface. Surv. Geophys. 33, 29–63. http://dx.doi.org/10.1007/s10712-011-9138-y.

Gebbers, R., Lück, E., Dabas, M., Domsch, H., 2009. Comparison of instruments for geoelectrical soil mapping at the field scale. Near Surf. Geophys. 7, 179–190. http://dx.doi.org/10.3997/1873-0604.2009011.

Gottfried, T., Auerswald, K., Ostler, U., 2012. Kinematic correction for a spatial offset between sensor and position data in on-the-go sensor applications. Comput. Electron. Agric. 84, 76–84.

Grellier, S., Florsch, N., Camerlynck, C., Janeau, J.L., Podwojewski, P., Lorentz, S., 2013. The use of Slingram EM38 data for topsoil and subsoil geoelectrical characterization with a Bayesian inversion. Geoderma 200–201, 140–155.

Lundgren, J., 2010. Splinefit(www.mathworks.com/matlabcentral/fileexchange/13812-splinefit) MATLAB Central File Exchange. (Retrieved November 11, 2013).
McNeill, J.D., 1980. Electrical conductivity of soils and rocks. Technical Note 5. Geonics Limited, Ontario.
Minsley, B.J., Smith, B.D., Hammack, R., Sams, J.I., Veloski, G., 2012. Calibration and filtering strategies for frequency domain electromagnetic data. J. Appl. Geophys. 80, 56–66.
Nielsen, M.L., 2012. Outlier detection and removal—Hampel(www.mathworks.com/matlabcentral/fileexchange/34795-outlier-detection-and-removal-hampel) MATLAB Central File Exchange. (Retrieved November 11, 2013).
Pearson, R.K., 2002. Outliers in process modeling and identification. IEEE Trans. Control Syst. Technol. 1063-6536 (10), 55–63.
Robinson, D.A., Lebron, I., Lesch, S.M., Shouse, P., 2004. Minimizing drift in electrical conductivity measurements in high temperature environments using the EM-38. Soil Sci. Soc. Am. J. 68, 339–345.
Saey, T., Delefortrie, S., Verdonck, L., De Smedt, P., Van Meirvenne, M., 2014. Integrating EMI and GPR data to enhance the three-dimensional reconstruction of a circular ditch system. J. Appl. Geophys. 101, 42–50. http://dx.doi.org/10.1016/j.jappgeo.2013.11.004.
Siemon, B., 2009. Levelling of helicopter-borne frequency-domain electromagnetic data. J. Appl. Geophys. 67, 206–218.
Simpson, D., Van Meirvenne, M., Saey, T., Vermeersch, H., Bourgeois, J., Lehouck, A., Cockx, L., Vitharana, U.W.A., 2009. Evaluating the multiple coil configurations of the EM38DD and DUALEM-21S sensors to detect archaeological anomalies. Archaeol. Prospect. 16, 91–102.
Smith, I.E., 2013. Hampel filter in C++. MATLAB Central File Exchange. (Retrieved November 11, 2013).
Sudduth, K.A., Drummond, S.T., Kitchen, N.R., 2001. Accuracy issues in electromagnetic induction sensing of soil electrical conductivity for precision agriculture. Comput. Electron. Agric. 31, 239–264.